Comparison of Elliptical and Triple-Spoke Cavities for the Rare Isotope Accelerator

V. Andreev, Y. Cho, C. Compton, M. Doleans, D. Gorelov, T.L. Grimm, W. Hartung,
M. Johnson, F. Marti, S. Schriber, X. Wu, R. C. York, and Q. Zhao
National Superconducting Cyclotron Laboratory
Michigan State University
East Lansing MI

January 30, 2004

TABLE OF CONTENTS

INTRODUCTION

The Rare Isotope Accelerator (RIA) driver linac specifications include acceleration of uranium ions up to 400 MeV/u and lighter ions to similar or higher energies with a total beam power of up to 400 kW. It is desirable to reach energies close to 1 GeV for protons. The baseline design of the high-energy section (β>0.4, E/A>85 MeV/u) of the driver linac uses 805 MHz elliptical cavities that were developed for the Spallation Neutron Source (SNS) [1,2]. Recently, Shepard et al [3,4] proposed an alternative design based on 345 MHz triple-spoke cavities claiming a number of advantages that support replacing the elliptical cavities with triple-spoke cavities in the RIA driver linac.

This paper provides an in-depth analysis of the accelerator design for the high-energy section of the RIA driver linac and uses this analysis to review the claims of Shepard et al [4]. The detailed analysis finds that the promised advantages of the triple-spoke are based on questionable assumptions and that several disadvantages were neglected. Also, a comparison of the status of cavity and cryomodule developments shows a significant difference in demonstrated performance. Finally it is shown that overall, the triple-spoke does not offer any credible advantage compared to elliptical cavities for RIA.

CAVITY DESIGN

The elliptical and triple-spoke cavity design parameters are given in Table 1 and drawings to the same scale are shown in Figure 1. Since no triple-spoke exists and the performance of triple-spokes can only be extrapolated from the double-spoke performance, the double-spoke parameters are also given Table 1. The design peak electric field, Ep, is 32.5 MV/m for the elliptical cavities and 27.5 MV/m for the triple-spoke cavities. The elliptical cavities can operate at a higher Ep because they were optimized for lower peak magnetic fields, Bp, of 70 mT or less, while the triple-spokes have a Bp of 83 mT or less. Design peak magnetic fields greater than 70 mT may be problematic for cw operation of the large triple-spoke cavities above 4 K. As an example the double-spoke cavity developed at Argonne National Laboratory (ANL) showed significant Q degradation when reaching levels of Bp close to 80 mT. Therefore thorough experimental verification is needed.

Type	**Six-cell elliptical**			**Triple-spoke**		**Double-spoke**
β_{opt}	0.49	0.63	0.83	0.50	0.62	0.393
f (MHz)	805			345		345
E_p**(MV/m)**	32.5			27.5		27.5
V_a**(MV)**	5.12	8.17	13.46	6.22	7.49	3.02
B_p**(mT)**	64.2	68.6	70.2	82.6	82.0	54.7
Length (m)	0.527	0.682	0.906	0.652	0.809	0.381
Aperture(m)	0.077			0.040		0.030
Diameter (m)	0.33			0.45		0.45
Mass (kg)	<105			<240		
Temperature (K)	2			4.5		4.2

Table 1. General cavity parameters (data for triple-spoke from [4]).

The cavities were designed to generate a maximum accelerating voltage, Va, at an optimum velocity, $c\beta_{opt}$. Because the structures are multi-gap, the voltage gain is effective over a limited range of velocities. Figure 2 shows the accelerating voltage versus β=v/c for the elliptical and triple-spoke cavities. The spoke cavities generate a larger voltage for β<0.59, while the elliptical cavities are more effective above this velocity. For acceleration of uranium to 400 MeV/u (corresponding to β=0.72), there is no advantage in adding the last elliptical cavity type (β_{opt} = 0.83), but it provides significantly higher energy protons due to its effectiveness at higher velocity. Since the β_{opt} = 0.83 elliptical cavity has already been developed, there is no technical risk and a minimal cost increase for a significantly higher proton energy. When comparing our Figure 2 with Figure 2 from reference [4], it should be noted that the Ep for the elliptical cavities assumed in that paper is 27.5 MV/m and not the 32.5 MV/m assumed in this paper, and the elliptical cavity β_{opt} values are not those used here.

Based on the design gradients and a synchronous phase of –30° for the elliptical and –25° for the triple-spoke, the number of cavities can be determined. The elliptical cavities are used after the second stripper accelerating U^{+87} to U^{+89} from 85 to 400 MeV/u. Though the triple-spokes are also proposed prior to the last stripper, the following discussion is focused on the region where the elliptical cavities are utilized. The number of cavities and cryomodules in the high-energy linac are given in Table 2. There are an additional 27 β=0.50 triple-spoke cavities (9 cryomodules) proposed at lower energies.

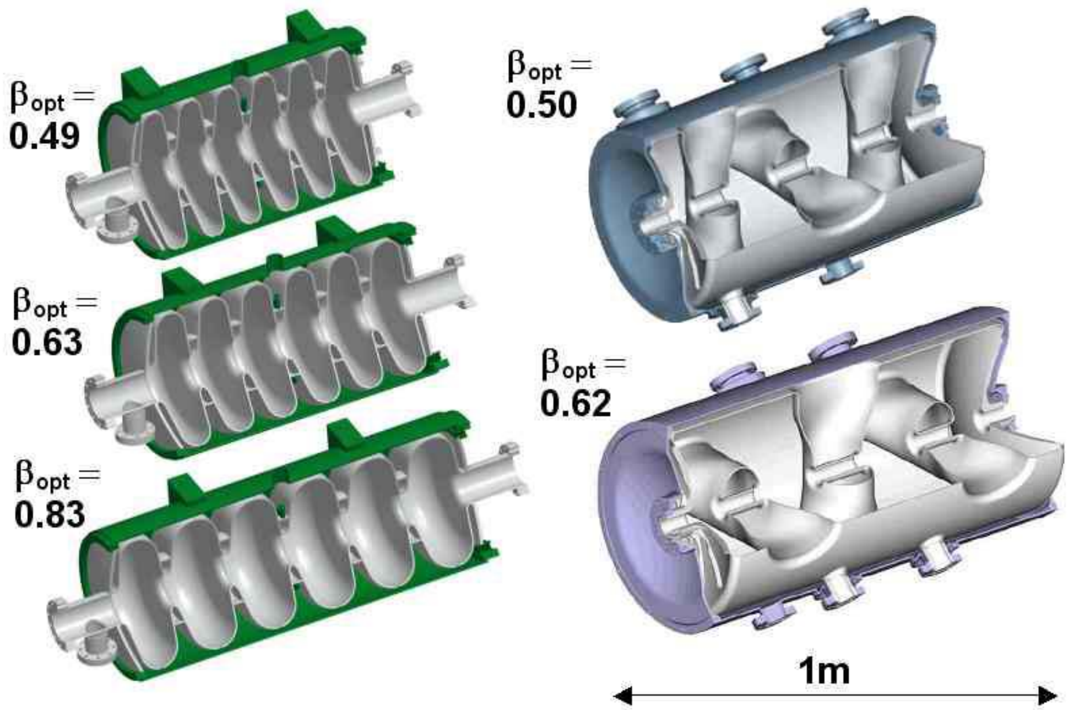

Figure 1. Baseline elliptical cavities (left) and proposed triple-spoke alternative [5] (right) with cavity β_{opt} values.

Given the design gradients of Table 1, there are 164 elliptical cavities in 41 cryomodules versus 138 triple-spoke cavities in 38 cryomodules. The elliptical cavities generate a higher energy proton beam of 1028 MeV compared to 956 MeV for the triple-spoke cavities.

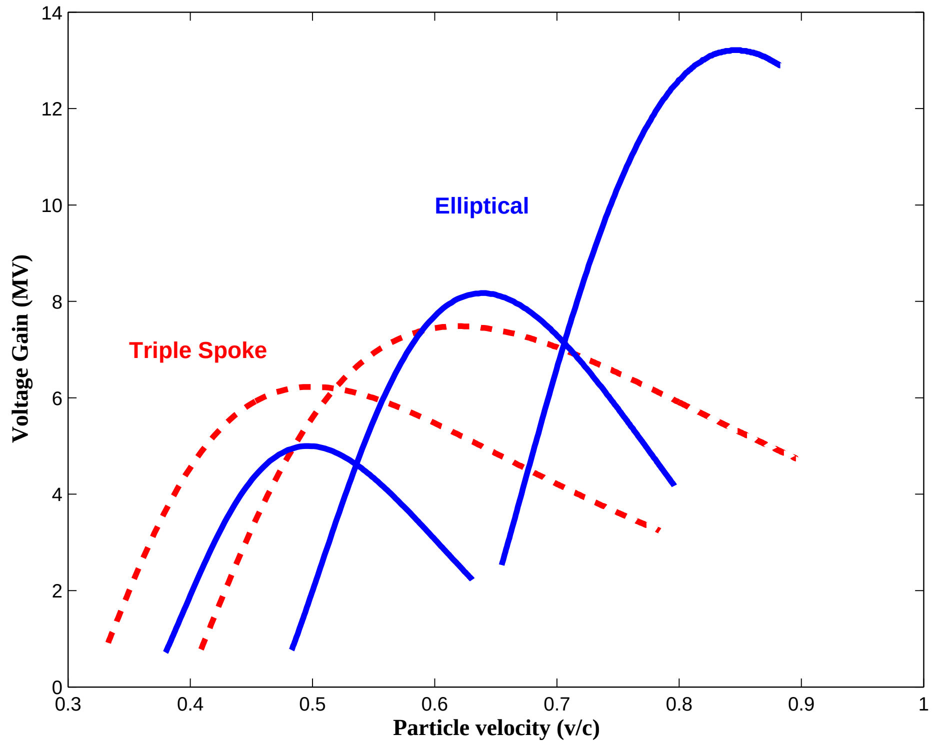

Figure 2. On axis accelerating voltage versus velocity for elliptical (solid lines) and triple-spoke (dashed lines) cavities with 32.5 and 27.5 MV/m peak electric field respectively.

Type	**Six-cell elliptical**			**Triple-spoke**	
β_{opt}	0.49	0.63	0.83	0.50	0.62
# cavities	68	64	32	42	96
Total # cavities	164			138	
# cryomodules	17	16	8	14	24
Total # cryomodules	41			38	
Maximum proton energy (MeV)	1028			956	

Table 2. Cavity and cryomodule count for acceleration of uranium from 85 to 400 MeV/u and maximum proton energy for the design gradients of Table 1.

EXPERIMENTAL VERIFICATION

The design values for Ep and Bp must be based on a thorough set of experimental data and should have reasonable safety factors to confidently assure linac performance. The simple shape of the elliptical cavities allows effective utilization of chemical processing and high pressure rinsing in a cleanroom environment. As a consequence elliptical cavities have reliably demonstrated maximum peak fields above 50 MV/m and 100 mT. On the other hand, the triple-spoke cavity has a small 4 cm aperture with a three-dimensional geometry that complicates chemical processing and high pressure rinsing. In addition, the triple-spoke has a larger 0.45 m diameter and a weight of about 240 kg making cavity handling more difficult.

It is essential that design values be based on prototyping and experimental data. Several copies of each elliptical cavity have been built and tested [6,7], but no triple-spokes have been built to date. Therefore, it is only possible to use data from the one double-spoke that has been built to extrapolate the triple-spoke performance [8].

The operating point Ep and Bp values for the elliptical cavities are based on the following considerations:

- The vertical tests of the β_{opt}=0.49, 0.63 and 0.83 cavities presented in Figure 3 show that *Qo* is approximately constant for Ep < 30 MV/m, with a maximum Ep of 41 to 56 MV/m and a maximum Bp of 87 to 110 mT.
- The design values for the SNS project are Ep = 35 MV/m and Bp = 75.6 mT at a *Q* of 5 x 10^9 for the β_{opt}=0.83 cavity.
- Design fields (Ep and Bp) for the CEBAF upgrade and TESLA cavities are significantly greater (42 MV/m and 72 mT for CEBAF and 47 MV/m and 102 mT for TESLA500).

Based on these considerations, Ep = 32.5 MV/m and Bp = 64-70 mT are judged to be appropriate design goals achievable with reasonable production protocols. These design values are shown in Figure 3 together with the results for the first multi-cell prototype of each elliptical cavity type to be used for RIA. Additional multi-cell cavities have been fabricated also. Two more 6-cell cavities for β_{opt} = 0.49 have been tested. Three more β_{opt} = 0.63 cavities have been tested after assembly into a prototype cryomodule for SNS [34]. All of these cavities have satisfied the design goals indicated in Figure 3.

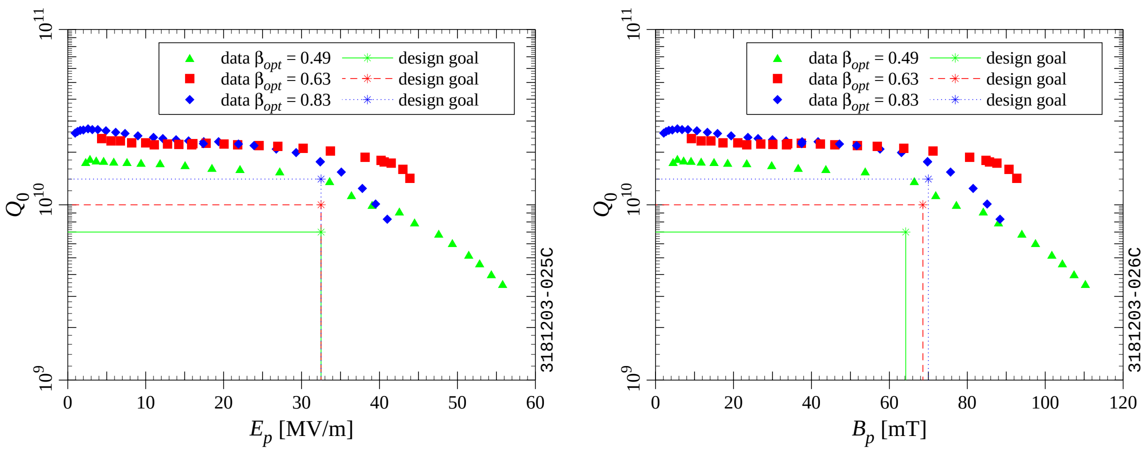

Figure 3. Experimental test results of the elliptical six-cell cavities for SNS [6] and RIA showing Q vs. Ep (left) and Q vs. Bp (right) at 2 K. The stars indicate the design values for RIA.

Shown in Figure 4 are the experimental results of the ANL double-spoke that will be used as guidance for the choice of operating point for the proposed triple-spoke. Although the design value for Ep (27.5 MV/m) is consistent with the experimental results for the double-spoke, the corresponding values for Bp (82 and 82.6 mT) are higher than the Bp obtained at 4.2 K. Based on past experience and the need for a safety factor, an appropriate design value for the triple-spoke would be Bp< 70 mT, a value that is consistent for comparison purposes with the methodology used to determine the operating parameters for elliptical cavities. Scaling the proposed design point to obtain Bp=70 mT results in Ep values of 23.3 and 23.5 MV/m for the triple-spokes of β_{opt}= 0.5 and 0.62, respectively. The corrected parameters for the triple-spoke are compared with the corresponding elliptical cavity parameters in Table 3. The lower values for the triple-spoke Ep and Bp results in basically the same number of cavities, but a larger number of triple-spoke cryomodules than for the elliptical units.

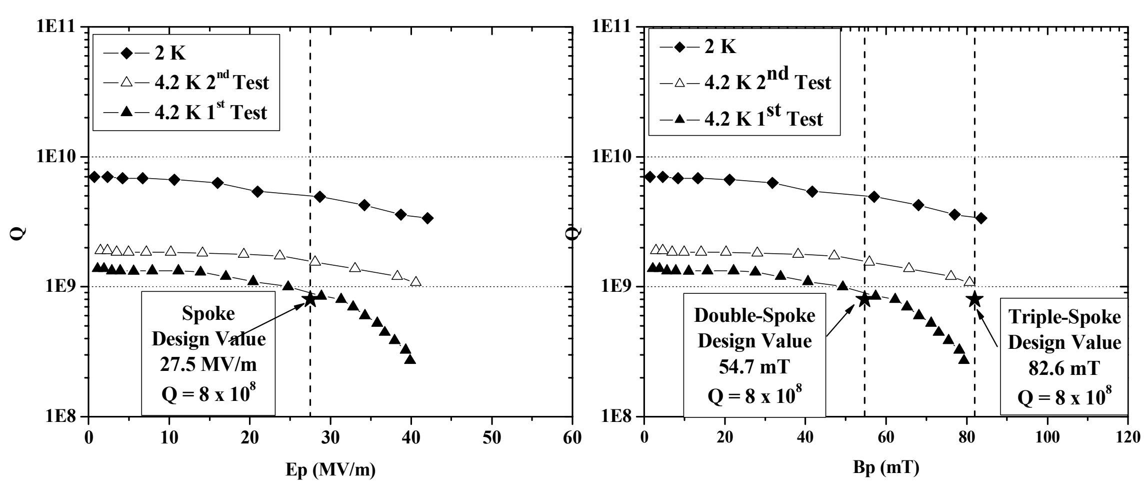

Figure 4. Double-spoke Q vs. peak electric (Ep) and peak magnetic (Bp) fields. Also shown are the proposed design values for the double and triple-spoke structures [5,8].

Beyond the one double-spoke cavity that has been fabricated so far, one can look to single-spoke cavity results for further guidance. A total of 5 single-spoke cavities have been fabricated and tested at Argonne [9], Los Alamos [10,11], and Orsay [12]. Good results have been obtained with these cavities, but none of them have reached the equivalent of the triple-spoke design goal (taking into account differing temperatures, geometry factors, and field ratios) indicated in Figure 4. This reinforces the concern that the proposed design values for the triple-spoke would be very difficult to achieve. All of the experimental results at T > 4 K indicate that the Q decreases as the field increases ("Q slope"), so that very low losses at high field are not realistic. Field emission is also seen in some of the measurements, which of course exacerbates the problem.

Type	**Six-cell elliptical**			**Triple-spoke**	
β_{opt}	0.49	0.63	0.83	0.50	0.62
Bp (mT)	64.2	68.6	70.2	70	70
Ep (MV/m)	32.5			23.3	23.5
Va(MV)	5.12	8.17	13.46	5.27	6.39
# cavities	68	64	32	51	112
Total # cavities	164			163	
# cryomodules	17	16	8	17	28
Total # cryomodules	41			45	

Table 3. General cavity parameters using experimentally verified peak fields and a safety margin.

BEAM DYNAMICS

To allow hands-on maintenance, the uncontrolled beam loss must be kept below 4 W/m along the linac [13]. This limits the fractional losses to $4x10^{-5}$/m at the entrance and $1x10^{-5}$/m at the exit of the high-energy linac. Uncontrolled losses can occur when either the transverse or longitudinal acceptance is exceeded, in which case it will appear as transverse loss. Controlled losses can be accommodated after the strippers using heavily shielded collimators that will already exist for removal of unwanted charge states.

Design values for misalignment, rf jitter and stripper foil thickness variation are accounted for in the simulations as listed in Table 4. The misalignments assume a Gaussian distribution with a cut-off at 2σ, while the rf jitter and stripper foil variations are a uniform distribution. Misalignments are corrected using beam position monitors, and steering magnets at the superconducting solenoids and room temperature quadrupoles.

	Section 1 0.3-13 MeV/u	Section 2 13-90 MeV/u	Section 3 85-400 MeV/u
σ for transverse misalignment of focusing elements	±0.25 mm	±0.5 mm	±1.0 mm
σ for transverse misalignment of cavities	±1.0 mm	±1.0 mm	±1.0 mm
Quadrupole skew	NA	NA	±2 mrad
RF jitter, maximum amplitude	±0.25 %	±0.5 %	±0.5 %
RF jitter, maximum phase	±0.25°	±0.5°	±0.5°
Stripper foil maximum thickness variation	±5 %		

Table 4. Design values for misalignment, rf jitter and stripper foil thickness variation. The strippers are located at the beginning of sections 2 and 3. The uranium energy loss at the second stripper will be from 3 to 5 MeV/u depending on the stripper thickness.

Transverse acceptance

Using both analytical and numerical methods, there have been extensive beam dynamics studies for both elliptical and triple-spoke cavity systems for the RIA driver linac [4,14,15,16,17]. The triple spoke lattice proposed in [4] uses solenoids as focusing elements with their 40 mm aperture cavities. A focusing lattice of either room temperature quadrupole doublets or superconducting solenoids would provide adequate focusing for the larger 77 mm aperture of the elliptical structures.

In the perfect accelerator, without misalignments, the acceptance of the triple-spoke lattice with superconducting solenoids is 35 π mm-mrad and the elliptical lattice acceptance is 130 π mm-mrad due to the different apertures. With room temperature quadrupole doublets, the elliptical lattice acceptance is 50 π mm-mrad.

The nominal transverse beam emittance at the entrance of the superconducting linac was 0.6 π mm-mrad (normalized, 99.5 %). Particle tracking using 100 random seeds was done with and without errors using DIMAD [18] (only transverse) and LANA [19] (transverse and longitudinal combined). The results from both codes agree very well. Consequently, the determination of the correction scheme was performed with DIMAD because of its higher speed, and the results were verified with LANA.

Without alignment and rf errors, but including stripper foil straggling and thickness variation, the beam emittance increased to 1.3 π mm-mrad at the entrance to section 3, and 1.6 π mm-mrad at the exit. Due to alignment and rf errors, the emittance of the beam grows. The maximum values calculated for 100 seeds were 3.2 π mm-mrad at the entrance to section 3, and 5.2 π mm-mrad at the exit.

In addition to the emittance growth, the misalignments cause the beam to move off-axis. The physical limitations are not the focusing elements but the cavity apertures, because the focusing elements have larger apertures. The comparison of beam size to cavity apertures is given in Table 5.

Figure 5 shows the transverse beam envelope for the triple-spoke lattice with solenoidal focusing, and Figure 6 shows the envelope for the elliptical cavity lattice with quadrupole focusing. The envelopes have been determined by choosing the maximum beam size at each position along the linac for all 100 seed simulations. These envelope calculations were used to determine the aperture to beam size ratio with errors in Table 5.

The elliptical structures with solenoidal focusing have the largest safety factor, but the quadrupole solution is also acceptable. As the quadrupole lattice uses room temperature magnets, it provides a reduced cost solution, easier alignment, higher reliability, easier maintenance, and less stringent stray magnetic field requirements. Due to these advantages we have chosen the quadrupole focusing option for the elliptical cavity lattice. Its reduced acceptance still exceeds that of the triple-spoke solution.

Lattice of Segment III of RIA Driver linac	**Cavity aperture (mm)**	**Aperture to Beam Size Ratio with Errors**
Elliptical Structures and Solenoidal Focusing	77	3.6
Elliptical Structures and Quadrupole Focusing	77	2.8
Triple-Spoke Structures and Solenoidal Focusing	40	1.9

Table 5. Cavity aperture and ratio of aperture to beam size with errors.

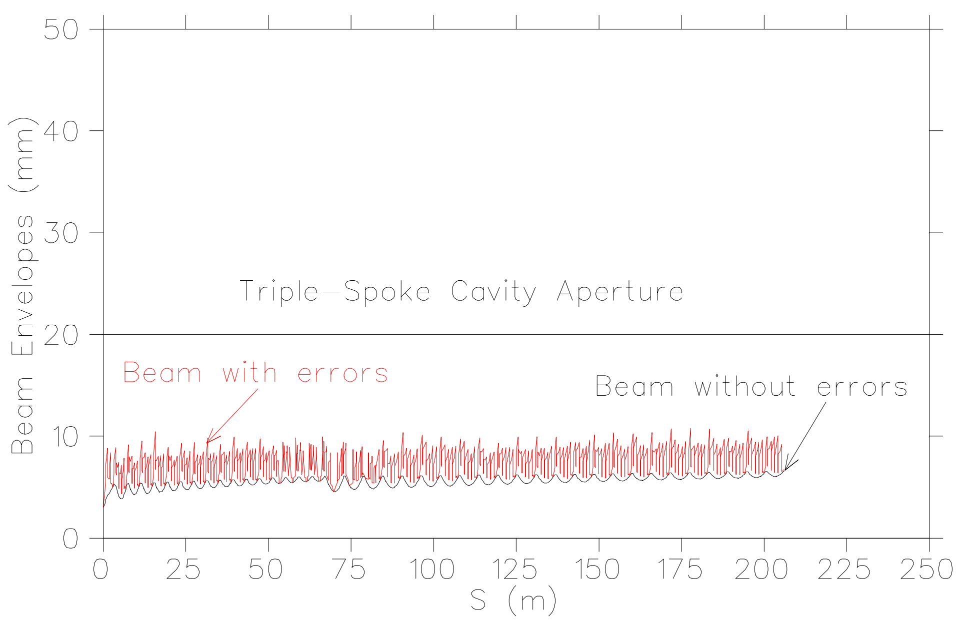

Figure 5. Transverse beam envelopes with and without errors for triple-spoke lattice with solenoidal focusing.

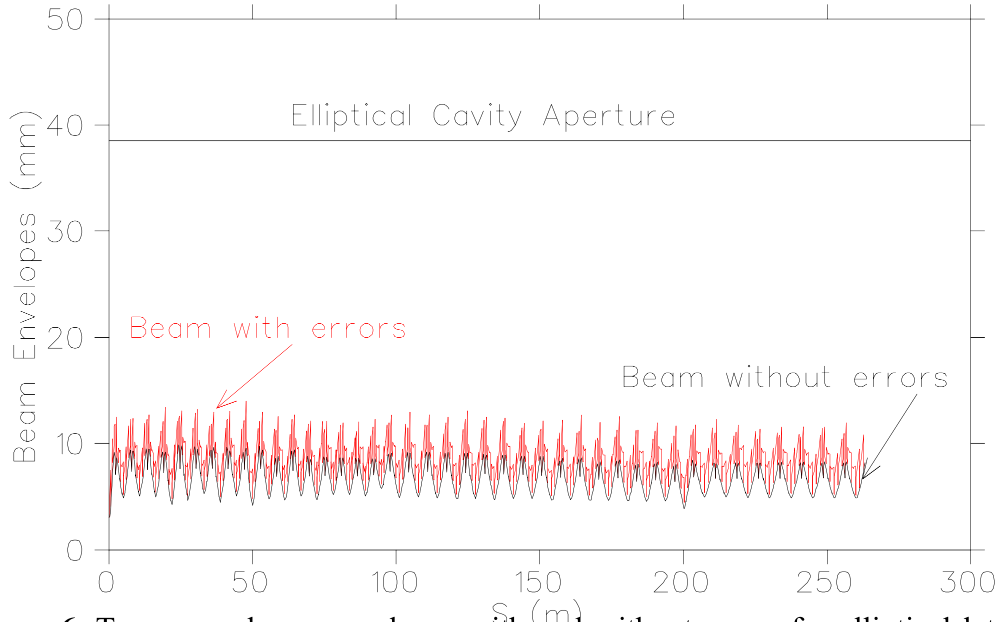

Figure 6. Transverse beam envelopes with and without errors for elliptical lattice with quadrupole focusing.

Longitudinal acceptance

Previous longitudinal and transverse beam dynamics studies at ANL and Michigan State University (MSU) showed adequate acceptance in the elliptical cavity linac with no inherent problems [17,20]. More recently ANL indicated that an elliptical cavity linac has serious flaws:

1. Parametric resonance will blow up the beam and cause unacceptable beam loss in the β_{opt}=0.49 section of the high-energy linac [21]**.**
2. The longitudinal acceptance is too small compared to the large beam emittance produced by multi-charge acceleration and stripper foil thickness variation [3,4].

With respect to the first claim, the coupling between the longitudinal and transverse motion in the presence of resonant conditions can lead to the parametric resonance and energy exchange resulting in the decrease or increase of the emittance in the different planes if the emittances were not equipartitioned initially. Extensive studies were conducted to investigate this issue [22]. The major focus for these studies was the beginning of the third section of the RIA driver linac consisting of the elliptical cavities with β_{opt}=0.49. They showed that the results of the simulation in [21] contradict the prediction of the theory based on the smooth approximation as well as the simulations in [22] that show no beam blow up. The discrepancy appears to be a misinterpretation in [21] of the longitudinal phase advance used. Therefore the recommendation by ANL to limit the number of cavities per cryostat in the beginning of section three of the RIA driver linac to 3, leading to an increase of the number of cryostats required, is unnecessary. The present design uses the same number of cavities per cryostat (4) in all of the third section.

In the second claim, the longitudinal emittance in ANL's simulation grows from ~2 π keV/u-ns at the exit of the RFQ to ~50 π keV/u-ns at the entrance to the elliptical cavity linac. Their calculated acceptance for the elliptical cavity linac is ~60 π keV/u-ns, which would be too close to the emittance for low loss operation, and thus not useable for RIA.

We explored the longitudinal phase space for the elliptical lattice by particle tracking with the computer code LANA [19]. Beginning with an initial emittance of 1.2 π keV/u-ns at the entrance of the superconducting linac (which is equivalent to 2 π keV/u-ns at the lower frequency of the ANL design), a longitudinal emittance at the entrance of the third and final linac segment of 16 π keV/u-ns was obtained using all 100 seeds. The effects of misalignments, rf phase and amplitude jitter, and stripper foil thickness variation as given in Table 4 were included. The longitudinal acceptance of the final segment using elliptical structures is 92.6 π keV/u-ns, giving an adequate ratio of acceptance to beam emittance of 5.8. The final emittance at the end of section 3 is 23 π keV/u-ns.

Confirming the adequacy of this ratio, no particle losses were found when tracking a larger longitudinal emittance of 35 π keV/u-ns using ten realizations (random seeds) of the linac, tracking 10^6 particles for each case. For a 40 π keV/u-ns emittance, 20-30 particles were lost for similar simulations, still within the beam loss criteria.

For the triple-spoke lattice the longitudinal acceptance of the final segment is about 280 π keV/u-ns, which is much larger than the input emittance of 16 π keV/u-ns calculated in our lattice for the first two sections, and also the 50 π keV/u-ns calculated in ANL's lattice [4]. Our simulations indicate that both options give adequate acceptance to beam emittance ratios and are summarized in Table 6 and Figure 7.

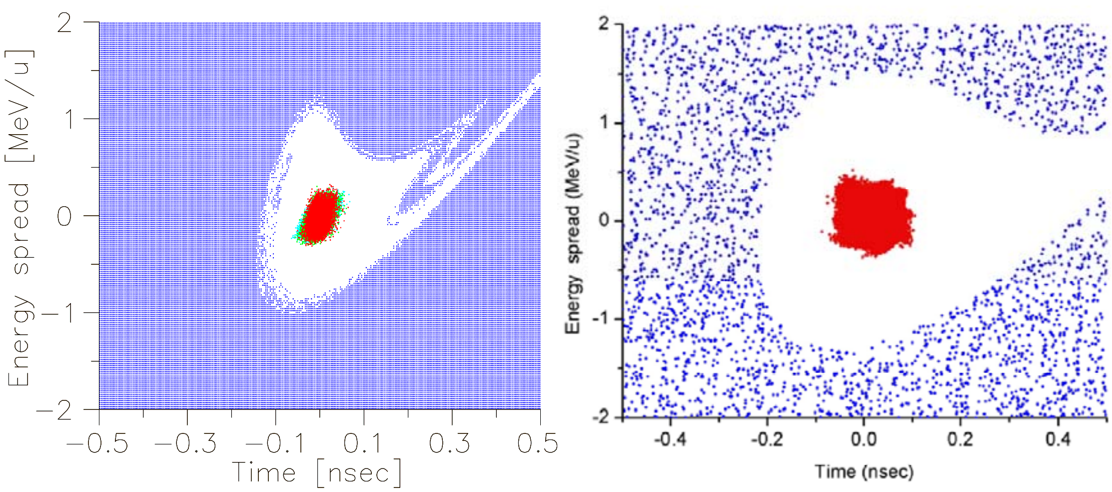

Figure 7. (Left) The elliptical lattice longitudinal acceptance and input beam emittance with an acceptance-to-emittance ratio of 5.8. (Right) The triple-spoke lattice longitudinal acceptance and input beam emittance with an acceptance-to- emittance ratio of 5.6 [4].

Our results predict a larger elliptical linac acceptance of 92.6 π keV/u-ns versus 60 π keV/u-ns as shown in [4]. This discrepancy is most likely due to the higher accelerating gradient (Ep=32.5 MV/m) and the closer spacing of the cavities and cryomodules as shown in Figure 10. Also, our simulations predict a smaller emittance of 16 π keV/u-ns compared with 50 π keV/u-ns from the ANL simulation. This difference comes primarily from ANL's larger rf jitter of ±1° and ±1 % in the lowest frequency cavities (58 MHz). The smaller values used in this paper are very reasonable for cavities (>80 MHz) whose microphonics are controlled by passive dampers and overcoupling [23]. This analysis shows that both elliptical and triple spoke linacs have adequate longitudinal acceptance, and a larger margin of safety is possible by decreasing the rf jitter.

Lattice of Section 3 of RIA Driver linac	**Input Longitudinal Emittance (99.5%) π keV/u ns**	**Longitudinal Acceptance π keV/u ns**	**Ratio of longitudinal acceptance to emittance**
Elliptical Cavities and Quadrupole Focusing	16	92.6	5.8
Triple-Spoke Cavities and Solenoidal Focusing	16/50	280	17.5/5.6

Table 6. Longitudinal emittance (with errors), acceptance and the ratio for the elliptical and triple-spoke lattices**.** The first value for the emittance of the triple spoke was calculated using our low and medium energy lattice. The second value corresponds to the ANL simulations [4].

CRYOGENIC REQUIREMENTS

The operating temperature of the triple-spoke cavities is to be 4.5 K according to one publication [3] and is 4.2 K in another publication [4]. Though the rf losses are obviously lower at 4.2 K, large-scale cryo-plants generally operate at a temperature higher than 4.2 K [24]. The operating temperature of choice for most low-frequency SRF accelerators is 4.5 K; this includes ALPI [25], CESR-III [26], JAERI Tandem Booster [27], KEK-B [28], LEP [29], and ATLAS [30]. Thus 4.5 K seems to be a more reasonable choice, and this is the operating temperature assumed in the following discussion for triple-spoke cavities.

The operating temperature and cryogenic load of the superconducting cavities were calculated to determine the required cryoplant capacity and cost. The dynamic heat load calculation used the following equations describing the power dissipated in a cavity, *Po*, in terms of the fundamental cavity parameters.

$$P_o = \frac{V_a^2}{R} = \frac{V_a^2}{\left(\frac{R}{Q}\right)Q} = \frac{V_a^2}{\left(\frac{R}{Q}\right)G} R_s = \frac{V_a^2}{\left(\frac{R}{Q}\right)G}\left(R_{BCS} + R_{res}\right)$$

$$R_{BCS} = 2\text{x}10^{-4}\frac{C_{RRR}}{T_K}\left(\frac{f_{GHz}}{1.5}\right)^2 \exp\left(-\frac{17.67}{T_K}\right)$$

where R is the linac definition of the shunt impedance, Q is the cavity quality factor, V_a is the accelerating voltage, G is the geometry factor, R_s is the total rf surface resistance, R_{BCS} is the BCS surface resistance, and R_{res} is the residual surface resistance. The BCS surface resistance is given in nΩ where f_{GHz} is the cavity frequency in GHz and T_K is the cavity temperature in K. The above equation describing R_{BCS} is obtained from [31]. The correction factor, C_{RRR}, ranges from 1 for reactor grade (RRR~25) niobium to 1.5 for high purity (RRR~250) niobium.

The power dissipation is inversely proportional to *(R/Q)G,* whose values are given in Table 7. The β_{opt}=0.63 and 0.83 elliptical cavities have a larger product than the triple-spokes, and thus are more efficient. The β_{opt}=0.49 elliptical cavity has a smaller product than the triple-spokes, but this is offset by operating at 2 K and because there are more high-β elliptical cavities in the linac.

Type	**Six-cell elliptical**			**Triple-spoke**		**Double-spoke**
$\boldsymbol{\beta_{opt}}$	0.49	0.63	0.83	0.50	0.62	0.393
f (MHz)	805			345		345
T(K)	2			4.5		4.2
R/Q(Ω)	173	279	483	494	520	474
G(Ω)	136	179	260	85.7	93.0	71
G·R/Q (kΩ^2)	23.5	49.9	126.0	42.3	48.4	33.7
E_{peak}(MV/m)	32.5			27.5		27.5
V_a(MV)	5.12	8.17	13.46	6.22	7.49	3.02
U (J)	29.9	47.2	74.2	36.1	49.8	8.9
$R_{BCS,min}$(nΩ)	4.2	4.2	4.2	46.3	46.3	37.5
$R_{res,min}$(nΩ)	5	5	5	5	5	5
Q_{max}	$1.5\text{x}10^{10}$	$2.0\text{x}10^{10}$	$2.8\text{x}10^{10}$	$1.7\text{x}10^{9}$	$1.8\text{x}10^{9}$	$1.7\text{x}10^{9}$
Q_{design}~1/2Q_{max}	$7\text{x}10^{9}$	$1.0\text{x}10^{10}$	$1.4\text{x}10^{10}$	$8\text{x}10^{8}$	$9\text{x}10^{8}$	$8\text{x}10^{8}$
P_{design}(W/cavity)	21.6	23.9	26.8	97.9	119.9	24.1

Table 7. Electromagnetic and cryogenic parameters (spoke data from [4, 8]).

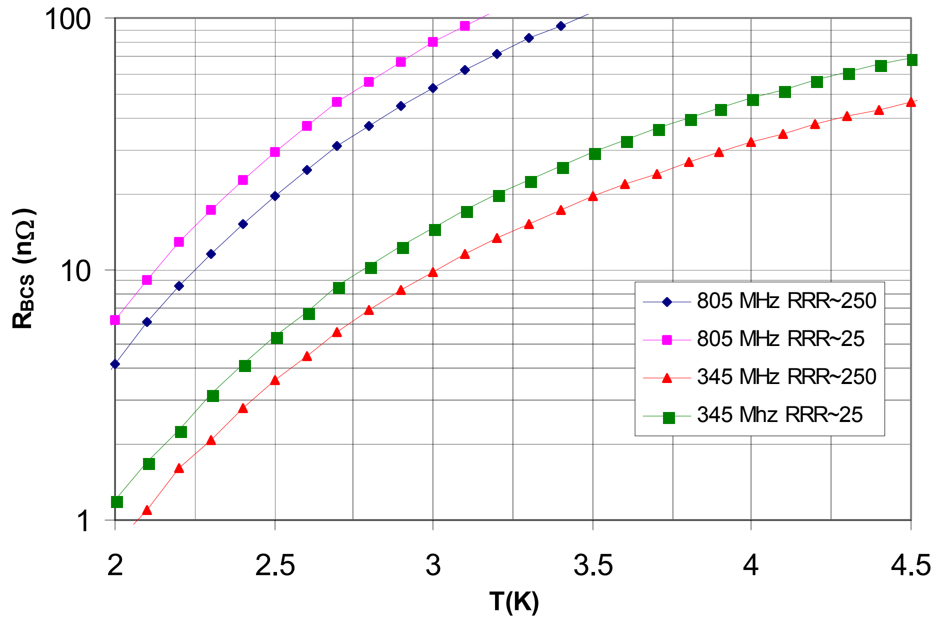

Figure 8. Range of R_{BCS} values resulting from varying RRR Nb values as a function of temperature (T) in K. The operating temperatures of the elliptical and triple-spoke cavities are 2 K and 4.5 K, respectively.

Since the accelerating voltage has already been determined, the only parameter left to quantify is the surface resistance, which can be broken down into a BCS and a residual component. The BCS component versus temperature is shown in Figure 8 for reactor grade (RRR~25) and high purity (RRR~250) niobium at 345 and 805 MHz. A lower BCS resistance can occur on the rf surface of high RRR niobium due to contamination (surface impurities), for example, from processing or bake-out. The elliptical cavities will operate at 2 K, giving a minimum BCS surface resistance of 4.2 nΩ, and the triple-spokes will operate at 4.5 K with a corresponding value of 46.3 nΩ. Therefore, the BCS component of the dissipated power is more than an order of magnitude larger for the triple-spokes at 4.5 K than elliptical cavities at 2 K.

The final parameter left to determine is the residual resistance. Well processed elliptical cavities can yield residual resistances of 2-10 nΩ [31]. As a design goal, we assume a residual resistance of 5 nΩ, which along with the BCS term, gives a minimum possible surface resistance. From this value a maximum possible Q, Q_{max}, is given in Table 7. Finally, a safety factor of 2 is used to obtain a Q_{design} that is half of Q_{max}. To verify that these are reasonable design values, the Q_{design} is compared with the prototype test results in Figure 3 and Figure 4. Since a triple-spoke has never been tested, the double-spoke results are used for comparison purposes.

Both elliptical and double-spoke prototype test results show Q_{design} developed by this methodology to have a reasonable safety factor, and are thus acceptable for determining the cryogenic load. The last row of Table 7 shows the power dissipated per cavity. The power dissipated per elliptical cavity is 22, 24, and 27 W for increasing β_{opt}, while the triple-spoke cavities generate 98 and 120 W per cavity for increasing β_{opt}. The elliptical cavities require less cryogenics, even taking into account Carnot efficiency and mechanical efficiencies of 18 % at 2 K and 30 % at 4.5 K [32].

The total cryoplant capacity for the high-energy linac segment (85-400 MeV/u) was calculated from the number of cavities with their design load, a 25 W static load per cryomodule, and a 50 % larger capacity plant for distribution and additional safety factor. Table 8 shows the required capacity, electrical usage and cost. The mechanical efficiency of the cryoplant is inferred from experience at CEBAF [32]. The capital cost of the cryo-plant is based on scaling laws for large cryo-plants [33] and converted to 2004 dollars. The elliptical cavity linac cryoplant is less than one-third the capacity required for the triple-spoke linac, but because it operates at 2 K, the plant electrical usage and cost are comparable to that of the triple-spoke linac.

Therefore, neither the elliptical or triple-spoke linacs offer an advantage in terms of cryoplant capacity or its capital and operating costs. The elliptical cavity option does offer a significant advantage since the 2 K superfluid reduces pressure fluctuations and concomitant microphonics compared to a 4.5 K system. The superfluid does not boil due to its large heat conductivity. The heat conductivity of the 4.5 K system is less and the large power dissipation of the triple-spoke cavities will cause significant boiling. Also, the operating pressure at 2 K is less than 25 torr with small fluctuations, while a 4.5 K system will operate above 760 torr with correspondingly larger pressure fluctuations.

Type	Six-cell elliptical	Triple-spoke
T(K)	2	4.5
Cryoplant Capacity (kW)	7.3	24.9
Cryoplant Electrical (MW)	6.1	5.4
Cryoplant Cost (M$)	18.1	18.5

Table 8. Cryogenic requirements for 85-400 MeV/u. The electrical power requirements are calculated with the assumption of a mechanical efficiency of 18% and 30% at 2 K and 4.5 K, respectively.

The analysis done in [4] claimed a factor of two lower refrigeration for the triple-spoke geometry by assuming an unreasonably large residual resistance. This was based on vertical test results for 14 early production cavities for SNS [34]. The decrease in Q at high field in these vertical tests was understood to be due to contamination during cavity preparation. The elimination of these contamination problems has been a priority for SNS. All three cavities in the prototype cryomodule had improved performance (relative to previous vertical tests) after assembly into the cryomodule and satisfied the RIA design goals given in Table 7 [34]. More recent results are also encouraging: the first 3 production cryomodules have been completed and tested, with results for 8 out of 9 cavities meeting the RIA design goals [35]. (The ninth cavity did not quite meet the design goal for RIA, as the Q was 9×10^9 instead of 1×10^{10} at Ep = 32.5 MV/m.) This indicates that the RIA design goals proposed in this paper can be achieved with production cavities under realistic conditions.

The cavities for TESLA [36,37] provide another proof of principle for operation of production cavities without field emission at fields above Ep = 32.5 MV/m. About 75 cavities have been fabricated by industry and tested at DESY so far. The cavity performance has improved over time during production. Using the recipe described above and taking into account the differences in frequency, geometry factor, and field ratios, the equivalent of the RIA design Q would be $9\text{x}10^9$ at Ea = 16.5 MV/m (Ep =33 MV/m, Bp= 70 mT) for the TESLA cavities. This goal is reached with a comfortable margin in the case of the third production series of TESLA cavities; however, a significant number of cavities would have been unable to reach this performance level in the first production series. Likewise, RIA will benefit from the experience gained during the production of SNS cavities.

The cavities for the CEBAF upgrade provide another point of reference. The design Q for these 7-cell elliptical cavities is $8\text{x}10^9$ at Ea = 19.2 MV/m (Ep =42 MV/m, Bp= 72 mT, Low Loss design) [38]. This goal is slightly more stringent than the design goal one would obtain on the basis of the recipe given above. Although no production cavities have been fabricated or tested yet, the experience with the CEBAF upgrade will likely be valuable for subsequent production of RIA cavities.

CRYOMODULE PERFORMANCE

The elliptical and triple-spoke cavity designs have been compared to determine the relative merits of their electromagnetic performance and cryogenic requirements. Because the driver linac is a significant element of the project cost and schedule, it is imperative before proceeding with production to mitigate technical risk by demonstrating prototype cryomodules performance under realistic operating conditions. In this regard, the relative maturity of the elliptical and triple-spoke systems designs was evaluated.

The basic cryomodule layout for both the elliptical and triple-spoke structures are similar with the cold mass hung from a top plate on alignment rails. This top plate and cold mass is either lowered into a box, or alternatively, the box is assembled around the cold mass. There are, however, a few major differences that are reviewed below. Cross sections of the cryomodules are shown in Figure 9 and Figure 10 [39].

Room temperature quadrupoles or superconducting solenoids

Because of the small triple-spoke aperture, high-field superconducting solenoids are required for the focusing lattice. Since the elliptical cavities have larger apertures, room temperature quadrupoles with their advantages are appropriate.

Cavity fabrication

The fabrication tolerances for elliptical cavities are well understood and within standard machine shop practices. Shrinkage and warpage due to electron beam welding is accounted for, and final frequency tuning with good field flatness is accomplished by plastically deforming individual cells using a simple tuning jig. This standard technique is used for CEBAF, TESLA and SNS multi-cell elliptical cavities.

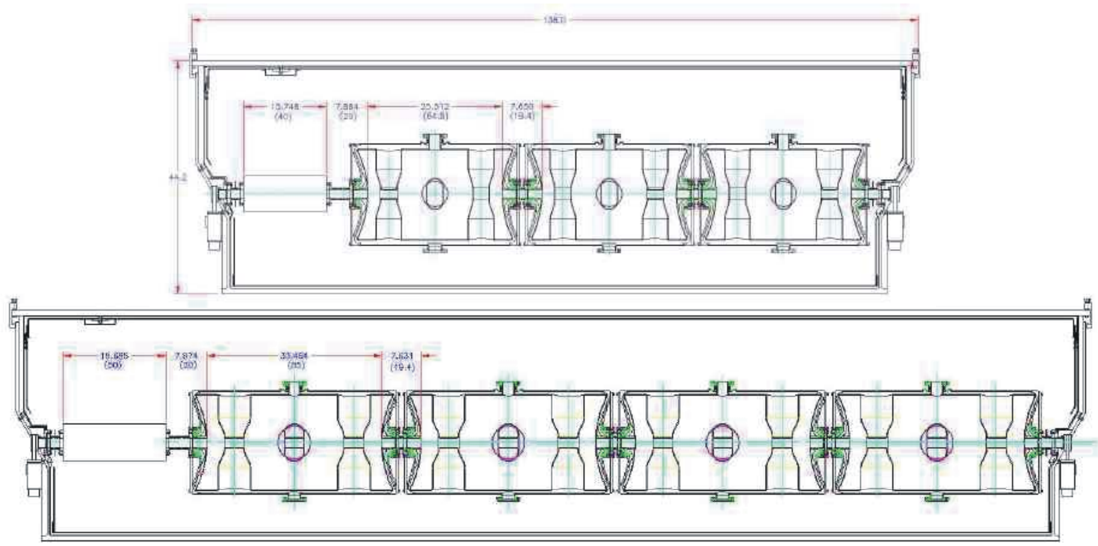

Figure 9. Triple spoke cryomodules from reference [5].

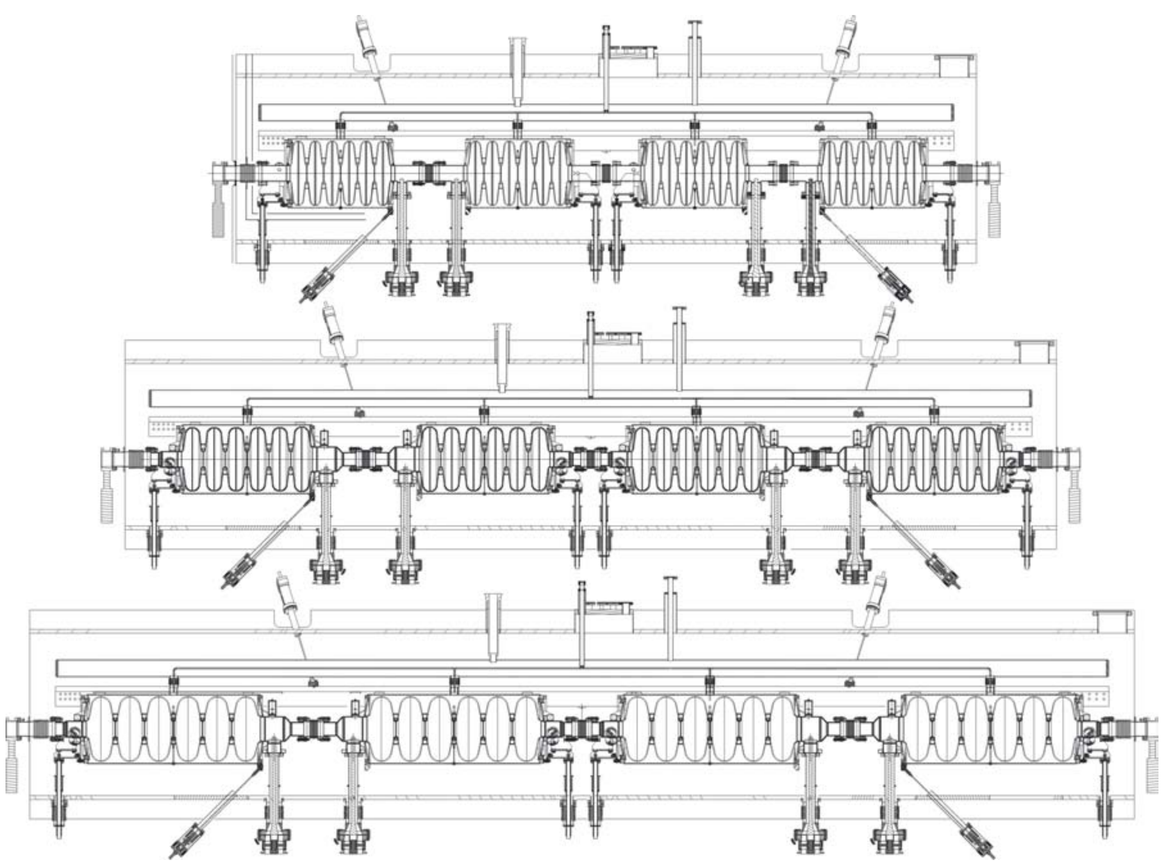

Figure 10. Elliptical cavity cryomodules.

The triple-spoke has strong cell-to-cell coupling, so field flatness is claimed not to be a problem. However, very tight mechanical tolerances will be required to obtain the desired operating frequency (345 MHz ± tuner bandwidth) since once a cavity has been formed, it is unclear how the center frequency will be retuned. Even with appropriate mechanical tolerance control, frequency retuning will be required each time a cavity is chemically etched. As an example, the double-spoke had a frequency of 347.6 MHz or 2.6 MHz over the design value and likely outside the range of a practical tuner.

The HOM analysis of the elliptical cavities has been performed [40]. Additional HOM couplers are not required for RIA because the large aperture of the elliptical structures lowers the cut-off frequency, allowing the higher order modes to leak out. No such analysis has been made for the triple-spoke cavities.

2 K versus 4.5 K operation

The use of 2 K superfluid for the elliptical cavities does not increase refrigeration loads or cost. The 2 K system offers significant advantages due to the quiescent nature of conduction heat transfer without boiling, and a low operating pressure with correspondingly small pressure fluctuations. The triple-spoke cavity design has attempted to minimize the vibration and frequency detuning due to boiling and pressure fluctuations of 4.5 K liquid helium by strengthening the end plates with gussets and thick reinforcements, but this will make cavity tuning more of a challenge.

Tuner – slow and fast

The elliptical cavities use a room temperature external tuner for slow (stepper motor) and fast (piezoelectric) frequency control. This same technique is proposed for the CEBAF upgrade that has similar bandwidth requirements [41]. It is unclear how the triple-spoke will be tuned for either slow or fast control, but its necessity is acknowledged [5]. Because the cavity has been made so rigid, the tuner may be a major challenge.

The use of a reactive or VCX tuner has been proposed for multi-spoke structures, but its use needs experimental verification for the high-β triple-spoke structures because of the relatively high frequency (345 MHz) and large stored energy, comparable to the elliptical cavities (see Table 7).

Vacuum manifold

Due to the small beam ports of the large triple-spoke cavities, an additional vacuum manifold is attached to the cavities inside the cryomodule along with a pumping system. This will complicate cleanroom assembly and increases the risk of contamination. The large aperture of the elliptical cavities allows pumping from the room temperature sections of the beam line where vacuum systems are already present.

Fixed versus moveable input rf coupler

The triple-spoke cavity is a half-wave structure and will experience multipacting barriers that must be conditioned. This conditioning process will require an adjustable input coupler with its added complexity and increased risk of contamination from moving parts. The elliptical cavities do not have problems with multipacting, and therefore can operate with simpler, less expensive fixed input rf couplers.

Cavity, cryomodule and tunnel cross-section

The triple-spoke cavity has a larger cross section, an additional vacuum manifold, and superconducting magnet leads that must be shielded from the cavity, all of which lead to a larger cryomodule and tunnel cross-section.

PROTOTYPE CRYOMODULE

A prototype β=0.49 two-cavity elliptical cryomodule is under construction and will be completed early in 2004. The two cavities have already been successfully tested in a vertical dunking Dewar with results similar to those presented earlier in this paper. Figure 11 shows the cavity with titanium helium vessel, power coupler and tuner. Cleanroom processing and assembly was completed at Jefferson Laboratory and shipped to MSU for installation into the cryomodule. Figure 12 shows the cold mass in the cleanroom ready for installation into the cryomodule, and Figure 13 shows the status of construction. The only steps remaining are installation of the magnetic and thermal shields, and welding the steel-box vacuum vessel. Testing under realistic operating conditions will proceed through the end of 2004.

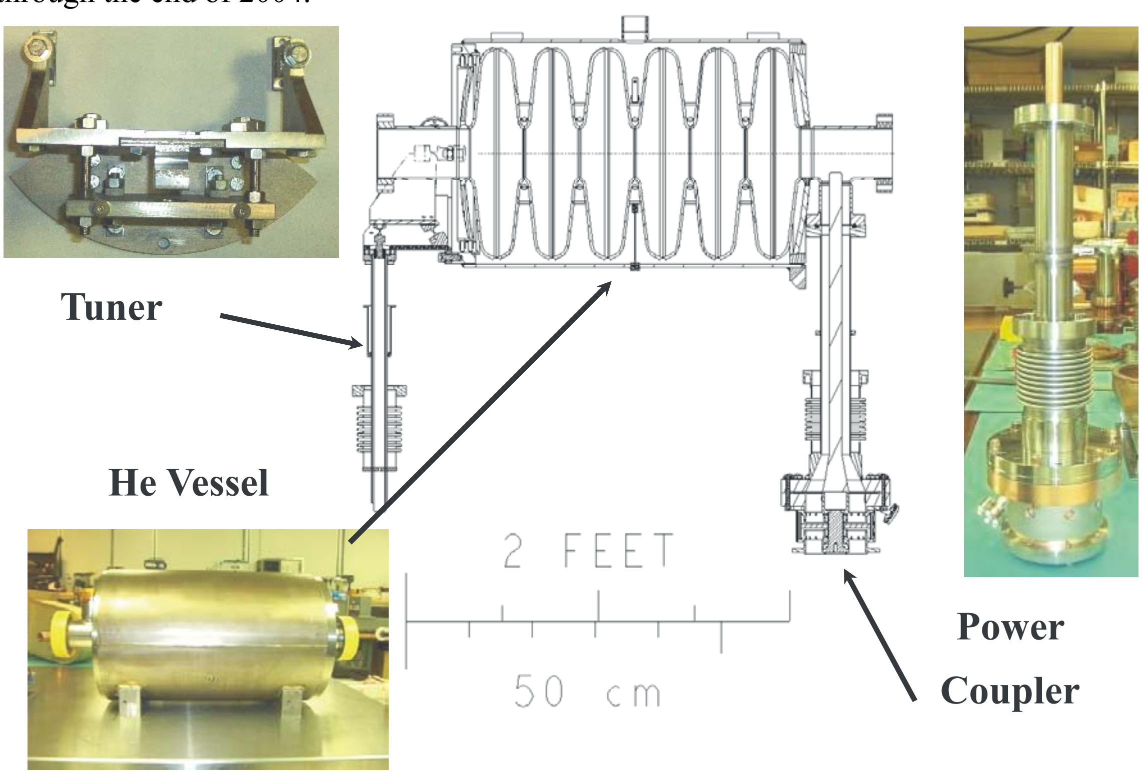

Figure 11. Six-cell β_{opt}=0.49 elliptical cavity with radial coupler ports, stiffening rings, helium vessel, tuner and input power coupler.

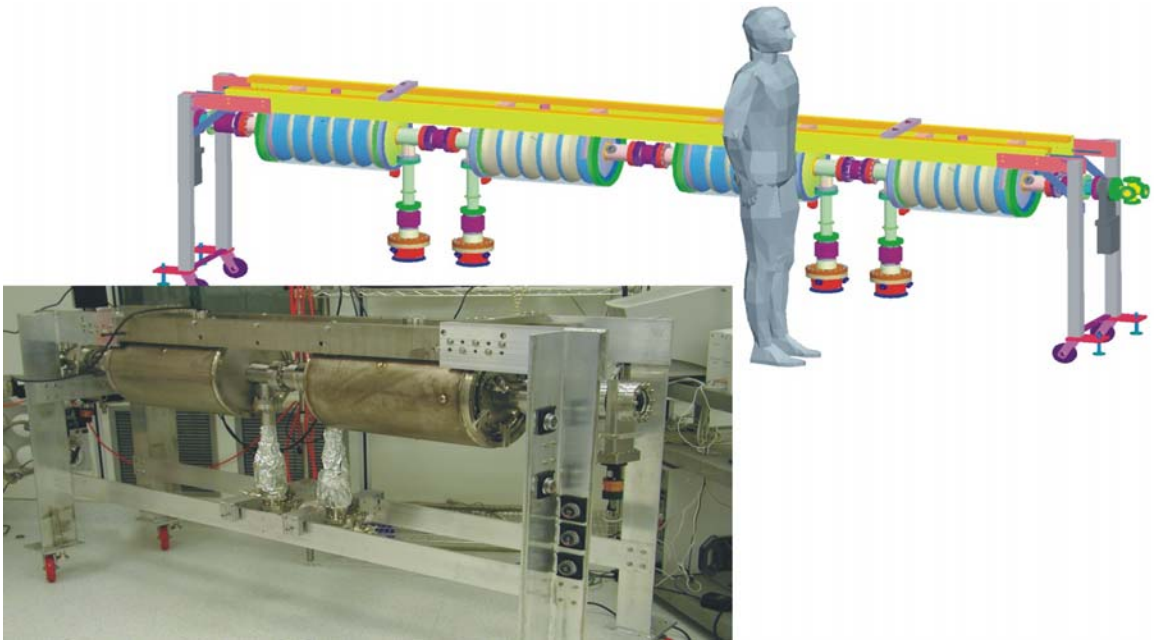

Figure 12. β_{opt}=0.49 elliptical cavity cold mass in cleanroom.

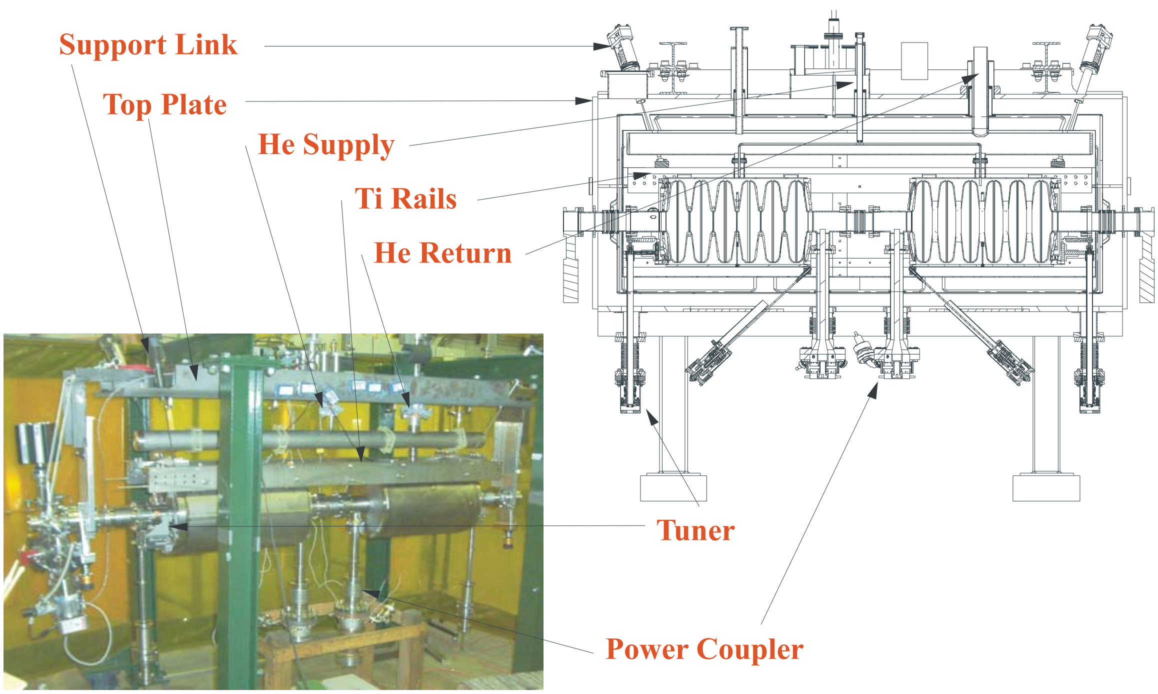

Figure 13. Status of the prototype β_{opt}=0.49 elliptical cryomodule (December 2003).

No triple-spoke cavity has been built, but prototypes of the β_{opt}=0.50 and 0.62 cavities are being fabricated and should be ready for testing in 2004. No plans have been presented for testing these prototype cavities in a cryomodule under realistic operating conditions (i.e. with superconducting solenoids, slow tuner, fast tuner, meeting alignment criteria, etc.). Construction of a prototype triple-spoke cryomodule would address many concerns like the need to have realistic longitudinal spacing that otherwise could degrade performance by:

a) Being difficult to assemble in a cleanroom environment without contaminating the rf surface due to tight spacing, tapped holes and trapped volumes.
b) Having no space for magnetic shielding that must reduce the stray field of the 9 T solenoids to 1-10 μT at the cavity during cool-down.
c) No space for tuner on end plates.

COST

Using SNS and RIA cost data and experience building the β_{opt}=0.49 prototype RIA elliptical cryomodule, a detailed cost estimate of the high-energy linac from 85-400 MeV/u has been done for the elliptical and triple-spoke options. The estimate includes all manpower, cryoplant, civil engineering and commissioning of this section of the driver linac.

A cost comparison of the β_{opt}=0.63 elliptical and β_{opt}=0.62 triple-spoke cryomodule is given in Table 9. Where triple-spoke designs were unavailable such as tuners and superconducting solenoids, the elliptical component designs were assumed. The triple-spoke cavity with helium vessel is significantly more expensive than the elliptical cavity due to larger quantities of niobium, more electron beam welding, and a more complicated helium vessel. The elliptical cavity costs are consistent with SNS and ACCEL cost estimates. Additional detailed breakdowns of the cost in Table 9 are available in reference [42].

The cryomodules proposed here for both the elliptical and triple-spoke linacs are less expensive than the SNS cryomodules. These savings come from the following differences:

a) CW operation allows the use of low power tetrodes instead of klystrons.
b) The lower power for the input coupler allows conduction cooling instead of He gas cooling.
c) The SNS cost includes HOM dampers, not included here.
d) The use of smaller He vessels
e) The rectangular (instead of circular) cryomodule simplifies the assembly.

Using the information of Table 9, the overall cost estimate for the high-energy linac section is given in Table 10. Assuming the higher value of 82 mT for the triple-spoke peak magnetic field, both linacs are comparable in cost. For a triple-spoke linac with a more realistic peak magnetic field of 70 mT, the cost for that option increases by about 17%, resulting in a *higher* cost for the triple-spoke option.

Components	Elliptical (β_{opt}=0.63)	Spoke (β_{opt}=0.62)
Cavity + He Vessel (4)	257	369
FPC (4)	88	92
Tuner (4)	24	24
Cleanroom Assembly	17	20
Support Frame	13	13
Top Plate	11	13
Vessel	11	17
Support Links	4	4
mu metal	24	31
Thermal	9	19
MLI	16	16
Vacuum Header	NA	5
Magnet	30	30
Misc.	52	50
Assembly	101	134
RF power (4)	574	574
Low-level RF (4)	27	27
Controls	20	20
TOTAL (k$)	**1,278**	**1,458**

Table 9. Cost comparison in k$ of the β=0.63 elliptical and β=0.62 triple-spoke cryomodules. The number of components is shown in parenthesis.

	Elliptical	Spoke
# Modules	**41**	**38**
Cryomodules RF, Magnet, & Controls	52,253	51,385
Cryoplant	18,100	18,500
Cryodistribution	5,000	5,000
Civil Engineering	30,000	30,000
Installation	5,000	5,000
Commissioning	20,000	20,000
Contingency (50%)	65,000	65,000
TOTAL (k$)	**195,353**	**194,885**

Table 10. Cost comparison for the elliptical and triple-spoke options of the high-energy driver linac from 85-400 MeV/u.

CONCLUSIONS

The baseline design of the high-energy section (β>0.4, E/A>85 MeV/u) of the RIA driver linac uses three 805 MHz elliptical cavity designs. The two highest β structures were developed for the SNS project. The lowest β structure has been developed for RIA. Prototype elliptical cavities have exceeded design requirements and demonstration of an elliptical cryomodule under realistic operating conditions will be completed in 2004. By then all major components of the high-energy linac will have been tested and ready for industrial production.

The proposed alternative based on triple-spoke cavities does not offer any credible advantage over elliptical cavities. Specifically, the merits of the elliptical design compared to the triple-spoke are summarized below, and show that the claims made by Shepard et al in [3,4,5] are not valid.

1. Prototypes of all elliptical cavity types have been tested and successfully exceeded design accelerating gradients and quality factors. First tests of a triple-spoke are anticipated in 2004.
2. The design peak magnetic field in the elliptical cavities is 70 mT, which is consistent with reliable cw operation and low cryogenic losses. The design value for the triple-spoke is 82 mT, which is problematic for cw operation of large cavities above 4 K. The triple-spoke design value should be decreased to 70 mT or less, which would increase the cavity and cryomodule count by over 17 %.
3. A prototype elliptical cryomodule including tuners, microphonics control and focusing elements that meet alignment criteria will be completed in early 2004 with testing through the end of 2004. No plans for similar testing of triple-spoke cryomodules have been presented.
4. The cryogenic requirement for the elliptical cavities is significantly less than that for the triple-spoke cavities (7 kW at 2 K versus 25 kW at 4.5 K). Also, the cryoplant cost and electrical usage for elliptical cavities with 2 K superfluid are comparable to that for triple-spokes at 4.5 K.
5. The overall cost estimate of the high-energy linac is nearly identical, ~$195M for both, using elliptical cavities (Bp=70 mT) and triple-spokes (Bp=82 mT). The larger number of elliptical cavities is compensated for by the higher cost of triple-spokes, which have fewer cavities per cryomodule, larger quantities of niobium, more electron beam welding, and a more complicated helium vessel. More realistic peak magnetic fields in the triple-spoke design will make that option more expensive than elliptical cavities.
6. The use of three elliptical cavity types generates a higher proton energy of 1028 MeV compared to 956 MeV for two types of triple-spokes. Since the three elliptical cavity types have already been developed, there is minimal risk to the schedule or cost of RIA.
7. Beam dynamics simulations have shown that both designs have adequate longitudinal and transverse acceptance, including alignment tolerances, rf jitter

and stripper foil thickness variation. While both linacs offer adequate acceptances, each has a slight advantage, with the elliptical having a larger transverse acceptance, and the triple-spoke having a larger longitudinal acceptance. The alignment tolerances of the elliptical focusing elements (room temperature quadrupoles) will be much easier to meet than the triple-spoke focusing elements (superconducting solenoids).

8. Operation with 2 K superfluid will greatly simplify operational stability and control of microphonics in elliptical cavities. The triple-spoke at 4.5 K must handle vibration induced by boiling as well as pressure fluctuations in the relatively high operating pressure of the cryoplant, both of which will produce microphonics or frequency fluctuations.

ACKNOWLEDGEMENTS
We would like to thank W. Chronis, P. Kneisel, P. Ostroumov, W. Schneider, K. Shepard and ACCEL for helpful discussions and information.

REFERENCES

[1] K. W. Shepard, J. R. Delayen, C. M. Lyneis, J. Nolen, P. Ostroumov, J. W. Staples, J. Brawley, C. Hovater, M. Kedzie, M. P. Kelly, J. Mammosser, C. Piller, M. Portillo, "SC Driver Linac for a Rare Isotope Facility," in *9th Workshop on RF Superconductivity: Proceedings* (1-5 November 1999, Santa Fe, New Mexico), Report LA-13782-C, Los Alamos National Laboratory, Los Alamos, New Mexico, 2000, p. 345-351.

[2] C. W. Leemann, "The Rare-Isotope Accelerator (RIA) Facility Project," in *Proceedings of the XX International Linac Conference* (21-25 August 2000, Monterey, California), Report SLAC-R-561, Stanford Linear Accelerator Center, Stanford, California, 2000, p. 331-335.

[3] K. W. Shepard, "Status of Low and Intermediate Velocity Superconducting Accelerating Structures," in *Proceedings of the 2003 Particle Accelerator Conference* (12-16 May 2003, Portland, Oregon), IEEE Publishing, p. 581-585.

[4] K. W. Shepard, P. N. Ostroumov, J. R. Delayen, "High-Energy Ion Linacs Based on Superconducting Spoke Cavities," *Phys. Rev. ST Accel. Beams* **6**, 080101 (2003).

[5] K. W. Shepard, "ANL Updates to the RIA Baseline Design," presented at the RIA R & D Workshop, 26-28 August 2003, Bethesda, Maryland.

[6] G. Ciovati, P. Kneisel, J. Brawley, R. Bundy, I. Campisi, K. Davis, K. Macha, D. Machie, J. Mammosser, S. Morgan, R. Sundelin, L. Turlington, K. Wilson, M. Doleans, S. H. Kim, D. Mangra, D. Barni, C. Pagani, P. Pierini, K. Matsumoto, R. Mitchell, D. Schrage, R. Parodi, J. Sekutowicz, P. Ylae-Oijala, "Superconducting Prototype Cavities for the Spallation Neutron Source (SNS) Project," in *Proceedings of the 2001 Particle Accelerator Conference* (18-22 June 2001, Chicago, Illinois), IEEE Publishing, Piscataway, New Jersey, 2001, p. 484-486.

[7] W. Hartung, C. C. Compton, T. L. Grimm, R. C. York, G. Ciovati, P. Kneisel, "Status Report on Multi-Cell Superconducting Cavity Development for Medium-Velocity Beams," in *Proceedings of the 2003 Particle Accelerator Conference* (12-16 May 2003, Portland, Oregon), IEEE Publishing, p. 1362-1364.

[8] J. D. Fuerst, M. Kedzie, M. P. Kelly, K. W. Shepard, E. Peterson, "Superconducting 345 MHz Two-Spoke Cavity for RIA," in *Proceedings of the 2003 Particle Accelerator Conference* (12-16 May 2003, Portland, Oregon), IEEE Publishing, Piscataway, New Jersey, 2003; M. P. Kelly, J. D. Fuerst, M. Kedzie, K. W. Shepard, "Cold Tests of the RIA Two-Cell Spoke Cavity," presented at the Eleventh Workshop on RF Superconductivity (8-12 September 2003, Travemünde, Germany).

[9] M. P. Kelly, K. W. Shepard, M. Kedzie, G. Zinkann, "Cold Tests of a Spoke Cavity Prototype for RIA," in *Proceedings of the 2001 Particle Accelerator Conference* (18-22 June 2001, Chicago, Illinois), IEEE Publishing, Piscataway, New Jersey, 2001, p. 1047-1049.

[10] T. Tajima, "Considerations of 2 K Operations," presented at the Workshop on the Advanced Design of Spoke Resonators (7-8 October 2002, Los Alamos, New Mexico).

[11] T. Tajima, R. L. Edwards, R. C. Gentzlinger, F. L. Krawczyk, J. E. Ledford, J.-F. Liu, D. I. Montoya, R. J. Roybal, D. L. Schrage, A. H. Shapiro, D. Barni, A. Bosotti, C. Pagani, G. Corniani, "Results of Two LANL β = 0.175, 350-MHz, 2-Gap Spoke Cavities," in *Proceedings of the 2003 Particle Accelerator Conference* (12-16 May 2003, Portland, Oregon), IEEE Publishing, Piscataway, New Jersey, 2003, p. 1341-1343.

[12] G. Olry, J.-L. Biarrotte, S. Blivet, S. Bousson, F. Chatelet, T. Junquera, A. Le Goff, J. Lesrel, C. Miélot, A. C. Mueller, H. Saugnac, P. Szott, "Development of SRF Spoke Cavities for Low and Intermediate Energy Ion Linacs," presented at the Eleventh Workshop on RF Superconductivity (8-12 September 2003, Travemünde, Germany).

[13] R. M. Ronningen, "Uncontrolled Beam Loss Estimates for Proton and Uranium Ion Beams in the Rare Isotope Accelerator LINAC", NSCL-RIA-2003-001, 2003.

[14] D. Gorelov, T. Grimm, W. Hartung, F. Marti, X. Wu, R. C. York, "Analysis of a Multi-Spoke Option for the RIA Driver Linac," in *Proceedings of the 2003 Particle Accelerator Conference* (12-16 May 2003, Portland, Oregon), IEEE Publishing, p. 2849-2851.

[15] X. Wu, D. Gorelov, T. Grimm, W. Hartung, F. Marti, R. C. York, "The Beam Dynamics Studies of Combined Misalignments and RF Errors for RIA," in *Proceedings of the 2003 Particle Accelerator Conference* (12-16 May 2003, Portland, Oregon), IEEE Publishing, p. 2972-2974.

[16] D. Gorelov, T. Grimm, W. Hartung, F. Marti, X. Wu, R. C. York, H. Podlech, "Beam Dynamics Studies at NSCL of the RIA Superconducting Driver Linac," in *Proceedings of EPAC 2002 Paris: Eighth European Particle Accelerator Conference* (3-7 June 2002, Paris, France), EPS-IGA/CERN, Geneva, Switzerland, 2002, p. 900-902

[17] P. N. Ostroumov, J. A. Nolen, K. W. Shepard, "Multiple-Charge Beam Dynamics in an Ion Linac," in *Proceedings of the XX International Linac Conference* (21-25 August 2000, Monterey, California), Report SLAC-R-561, Stanford Linear Accelerator Center, Stanford, California, 2000, p. 1018-1022; P. N. Ostroumov, "Development of a Medium-Energy Superconducting Heavy-Ion Linac," *Phys. Rev. ST Accel. Beams* **5**, 030101 (2002).

[18] R. Servranckx, K. Brown, L. Schachinger and D. Douglas, "User's Guide to the Program DIMAD", SLAC report 285, UC-28, May 1985.

[19] Dmitry V. Gorelov, Peter N. Ostroumov, "Application of LANA Code for Design of Ion Linac," in *Proceedings of the Fifth European Particle Accelerator Conference* (10-14 June 1996, Sitges, Spain), Institute of Physics, Bristol, UK, 1996, p. 1271.

[20] D. Gorelov, J. Kim, F. Marti, H. Podlech, X. Wu, R. York, "Superconducting Driver Linac Beam Dynamics Optimization for RIA," in *Proceedings of the 2001 Particle Accelerator Conference* (18-22 June 2001, Chicago, Illinois), IEEE Publishing, Piscataway, New Jersey, 2001, p. 4086-4088.

[21] P. N. Ostroumov, "Design Features of High-Intensity Medium-Energy Superconducting Heavy-Ion Linac," in *Proceedings of Linac 2002: XXI International Linear Accelerator Conference*, (19-23 August 2002, Gyeongju, Korea) Pohang Accelerator Laboratory, Pohang, Korea, 2002, p. 64-66.

[22] R. Duperrier, D. Gorelov, "Instabilities Study and Implications for the RIA Project," in *Proceedings of the 2003 Particle Accelerator Conference* (12-16 May 2003, Portland, Oregon), IEEE Publishing, p. 2805-2807.

[23] A. Facco, "High Gradient Locking of Beam Loaded QWRs", presented at *RIA Driver Workshop II*, May 2002, ANL.

[24] C. Rode, R. Ganni, in *Handbook of Accelerator Physics and Engineering*, Alexander Wu Chao & Maury Tigner, Editors, World Scientific, Singapore, 1999, p. 322-328.

[25] A. M. Porcellato, G. Bisoffi, A. Facco, S. Gustafsson, I. I. Kulik, A. Lombardi, V. Palmieri, V. L. Ruzinov, S. Y. Stark, V. Andreev, G. Bassato, A. Battistella, M. Bellato, G. Bezzon, S. Canella, M. Cavenago, F. Cervellera, A. Dainelli, P. Favaron, G. Fortuna, M. F. Moisio, R. Pengo, A. Pisent, M. Poggi, F. Scarpa, J. S. Sokolowski, V. Zvyagintsev, F. Chiurlotto, L. Badan, L. Bertazzo, A. Beltramin, L. Boscagli, D. Carlucci, T. Contran, A. Dainese, M. De Lazzari, F. Poletto, R. Preciso, F. Stivanello, L. Ziomi, "Status of RF Superconductivity at L. N. L.," in *Proceedings of the Seventh Workshop on RF Superconductivity* (17-20 October 1995, Gif sur Yvette, France), Report CEA/Saclay 96 080/1, Saclay, Gif sur Yvette, France, 1996, p.43-45.

[26] S. Belomestnykh, P. Barnes, E. Chojnacki, R. Ehrlich, R. Geng, D. Hartill, R. Kaplan, J. Knobloch, H. Padamsee, S. Peck, P. Quigley, J. Reilly, D. Rubin, D. Sabol, J. Sears, V. Veshcherevich, G. Werner, "Operating Experience with Superconducting RF at CESR and Overview of Other SRF Related Activities at Cornell University," in *9th Workshop on RF Superconductivity: Proceedings* (1-5 November 1999, Santa Fe, New Mexico), Report LA-13782-C, LANL, Los Alamos, New Mexico, 2000, p. 24-30.

[27] S. Takeuchi, M. Matsuda, "First Three Year Operational Experience with the JAERI Tandem-Booster," in *Proceedings of the Eighth Workshop on RF Superconductivity* (6-10 October 1997, Abano Terme, Italy), Report LNL-INFN (Rep) 133/98, Laboratori Nazionali di -Legnaro, Legnaro (Padova), Italy, 1998, p. 237-247.

[28] S. Belomestnykh, "Operating Experience with β = 1 High Current Accelerators," presented at the Eleventh Workshop on RF Superconductivity (8-12 September 2003, Travemünde, Germany).

[29] P. Brown, O. Brunner, A. Butterworth, E. Ciapala, H. Frischholz, G. Geschonke, E. Peschardt, J. Sladen, "Performance of the LEP200 Superconducting RF System," in *9th Workshop on RF Superconductivity: Proceedings* (1-5 November 1999, Santa Fe, New Mexico), Report LA-13782-C, LANL, Los Alamos, New Mexico, 2000, p. 1-5.

[30] Richard Pardo, Gary Zinkann, "Long-Term Operating Experience for the ATLAS Superconducting Resonators," in *9th Workshop on RF Superconductivity: Proceedings* (1-5 November 1999, Santa Fe, New Mexico), Report LA-13782-C, LANL, Los Alamos, New Mexico, 2000, p. 10-14.

[31] Hasan Padamsee, Jens Knobloch, Tom Hays, *RF Superconductivity for Accelerators*, John Wiley & Sons, New York, 1998.

[32] W. J. Schneider, P. Kneisel, C. H. Rode, " Gradient Optimization for SC CW Accelerators", *Proceedings of the 2003 Particle Accelerator Conference* (12-16 May 2003, Portland, Oregon), IEEE Publishing, p. 2863-2865.

[33] R. A. Byrns, M. A. Green, "An Update on Estimating the Cost of Cryogenic Refrigeration," Report LBNL-40188, Lawrence Berkeley National Laboratory, Berkeley, California, 1997.

[34] J. Preble, I. E. Campisi, E. Daly, G. K. Davis, J. R. Delayen, M. Drury, C. Grenoble, J. Hogan, L. King, P. Kneisel, J. Mammosser, T. Powers, M. Stirbet, H. Wang, T. Whitlatch, M. Wiseman, "SNS Cryomodule Performance," in *Proceedings of the 2003 Particle Accelerator Conference* (12-16 May 2003, Portland, Oregon), IEEE Publishing, p. 457-461.

[35] C. H. Rode, "JLAB Overview," presented at the SNS Advisory Committee Review, Oak Ridge, TN (22-24 September 2003).

[36] H. Weise, "Superconducting RF Structures Test Facilities and Results," in *Proceedings of the 2003 Particle Accelerator Conference* (12-16 May 2003, Portland, Oregon), IEEE Publishing, p. 673-677.
[37] K. Zapfe, "Activities at DESY with High Gradient Superconducting RF Cavities for e^-/e^+ Linear Accelerators," presented at the Eleventh Workshop on RF Superconductivity (8-12 September 2003, Travemünde, Germany).
[38] Leigh Harwood, "Upgrading CEBAF to 12 GeV," in *Proceedings of the 2003 Particle Accelerator Conference* (12-16 May 2003, Portland, Oregon), IEEE Publishing, Piscataway, New Jersey, 2003, p. 586-588.
[39] T. L. Grimm, W. Hartung, M. Johnson, R. C. York, P. Kneisel, L. Turlington, "Cryomodule Design for the Rare Isotope Accelerator," in *Proceedings of the 2003 Particle Accelerator Conference* (12-16 May 2003, Portland, Oregon), IEEE Publishing, p. 1350-1352.
[40] T. L. Grimm, W. Hartung, F. Marti, H. Podlech, R. C. York, J. Popielarski, C. Wiess, L. Kempel, G. Ciovati, P. Kneisel, "Input Coupling and Higher-Order Mode Analysis of Superconducting Axisymmetric Cavities for the Rare Isotope Accelerator," in *Proceedings of EPAC 2002 Paris: Eighth European Particle Accelerator Conference* (3-7 June 2002, Paris, France), EPS-IGA/CERN, Geneva, Switzerland, 2002, p. 2241-2243.
[41] G. Davis, J. Delayen, M. Drury, E. Feldl, "Development and Testing of a Prototype Tuner for the CEBAF Upgrade Cryomodule," in *Proceedings of the 2001 Particle Accelerator Conference* (18-22 June 2001, Chicago, Illinois), IEEE Publishing, Piscataway, New Jersey, 2001, p. 1149-1151.
[42] C. C. Compton, M. Johnson, L. L. Saxton, J. Vincent "Cost Estimate of the High Energy Driver Linac for RIA" internal report, NSCL-RIA-2003-002, 2003.